Am J Transl Res 2021;13(9):10112-10126
www.ajtr.org /ISSN:1943-8141/AJTR0133200

Original Article

CircMYC regulates the mitochondrial respiration and cell viability *via* miR-516a-5p/AKT3 axis in acute myeloid leukemia

Xueqin Zou[1], Min Jiang[2]

[1]*Health Management Center,* [2]*Department of Pediatrics, Shenzhen University General Hospital, Shenzhen 518055, Guangdong Province, China*

Received March 16, 2021; Accepted July 24, 2021; Epub September 15, 2021; Published September 30, 2021

Abstract: Objective: Acute myeloid leukemia (AML) is a hematological malignancy with an aberrant proliferation of immature myeloid cells. This study aimed at exploring the regulatory function of circMYC in AML progression. Methods: Expression levels of CircMYC, miR-516a-5p, AKT3 and apoptosis-related proteins were determined by RT-qPCR and western blot. Cell viability and proliferation were examined by CCK8 assay and EdU assay. Annexin V/PI staining was used to assess cell apoptosis. Mitochondrial respiration function was confirmed by oxygen consumption rate (OCR). The relationships among circMYC, miR-516a-5p and AKT3 were detected by dual-luciferase reporter (DLR) assay, RNA-pull down assay and RNA immunoprecipitation (RIP) assay, respectively. Results: CircMYC was positively correlated with poor prognosis in AML patients (all $P<0.05$). Knockdown of circMYC decreased cell viability and OCR but increased cell apoptosis rates (all $P<0.05$), and miR-516a-5p overexpression displayed the similar trend. Mechanistically, the oncogenic effects of circMYC were achieved by sponging miR-516a-5p and increasing AKT3. Conclusion: Decreased expression of circMYC could suppress AML progression by regulating miR-516a-5p/AKT3, suggesting a new therapeutic target in AML treatment.

Keywords: Cell apoptosis, mitochondrial respiration, circMYC, AML, miR-516a-5p, AKT3

Introduction

As a malignant hematopoietic disease, acute myeloid leukemia (AML) is associated with rapid division and proliferation of immature myeloid immune cells [1]. According to French-American-British (FAB) classification, AML were divided into five subtypes, including M1-M5 [2]. Among those, only AML-M3 has achieved a high cure rate by the combination treatment of arsenic trioxide (As_2O_3) and all-trans retinoic acid. The therapeutic efficacy of other types of AML is still unsatisfactory [3]. Currently, the main treatment approaches for other types of AML are radiotherapy, chemotherapy and allogeneic bone marrow transplantation (allo-BMT) [4]. However, due to the occurrence of chemotherapy resistance and the limited supply of bone marrow transplantation, the five-year survival rate is only about 30% [5]. Therefore, it is of great significance to develop novel targeted therapeutic drugs for AML.

With the development of bioinformatics, the vital role of non-coding RNAs (ncRNAs) in tumor therapy, including microRNAs (miRNAs), circular RNAs (circRNAs) and long noncoding RNAs (lncRNAs) has been widely investigated [6]. MiRNAs are endogenous non-coding single stranded small RNAs with 21-23 bases in length, and was reported to regulate the progression of AML [7]. Moreover, specific miRNAs are also identified as biomarkers of AML, and used in the diagnosis and prognosis prediction [8]. In addition, miRNAs play their roles in tumor cells by acting with its downstream mRNA [9]. For example, miR-212-5p targeted FZD5 and inhibited the proliferation of AML cells [10]. What's more, circRNAs can regulate mRNA expression by sponging miRNAs. CircRNA-miRNA-mRNA network can be a potential therapeutic strategy for many kinds of tumors, including AML [11]. For example, it is reported that circMYC was associated with the recurrence and chemotherapy-resistance in myeloma [12].

Table 1. The squence of reagents used in cell transfection

	Sequence
miR-516a-5p mimics	5'-UUCUCGAGGAAAGAAGCACUUUC-3'
miR-NC	5'-UCGCUUGGUGCAGGUCGGGAA-3'
miR-516a-5p inhibitor	5'-GAAAGTGCTTCTTTCCTCGAGAA-3'
inhibitor NC	5'-UUCUCCGAACGUGUCACGUTT-3'
circMYC-WT	5'-UGGCUCCCCCUCCUGCCUCGAGAA-3'
circMYC-MUT	5'-UGGCUCCCCCUCCUGCGAGCUCUA-3'
AKT3-WT	5'-AUAUCACAUGUGGAUGUCGAGAC-3'
AKT3-MUT	5'-AUAUCACAUGUGGAUGAGCUCUC-3'

CircMYC overexpression promoted cell proliferation and reduced radiosensitivity in tumor cells [13]. However, the mechanism of circMYC function in AML is still unknown. In our research, we examined the effect of circMYC on regulating the cell functions of peripheral blood mononuclear cells as well as its underlying mechanisms, in order to provide new molecular target for the treatment of AML.

Materials and methods

Cell culture and transfection

The experiments were authorized by the hospital ethics committee. Informed consents had been obtained before experiment. The peripheral blood mononuclear cells (PBMCs) derived from clinical AML patients or healthy donors (NC) were extracted from fresh blood by Ficoll density gradient centrifugation. Human AML cell lines including HL60, THP-1, U937 and KG1, and the normal bone marrow stomal cell line HS5 were all collected from American Type Culture Collection (ATCC) and incubated with DMEM medium (Gibco, Grand Island, USA) containing 12% fetal bovine serum (FBS, Gibco). The culture conditions of 37°C with 5% CO_2 were used for all types of cells. For circMYC knockdown, lentiviral vectors containing circMYC shRNA were transfected into cells, and the shRNA negative control (NC) was used in control group. For overexpression or knockdown of miRNAs, miR-516a-5p mimics or miR-516a-5p inhibitor, and miR-NC or inhibitor NC were used, respectively. For overexpression of AKT3, the AKT3 pcDNA3.1 plasmid was established. For dual-luciferase report (DLR) assay, the sequences of circMYC or AKT3 containing the binding sites (including wide type and mutation type) to miR-516a-5p were established. The above sequences are shown in **Table 1**. For RNA pull down assay, cell lysates were incubated with Bio-miR-516a-5p, Bio-circMYC, and Bio-miR-520h. The materials were purchased from Genepharm company (Suzhou, China).

Quantitative reverse transcription PCR (RT-qPCR)

A TRIzol reagent (Invitrogen) was used for collecting the total RNA from cells. After that, the reverse transcriptions of RNA into cDNA were conducted through a reverse transcriptase kit (Invitrogen). The used primers are shown in **Table 2**. PCR processes were conducted on ABI 7500 real-time PCR system. Using the $2^{-\Delta\Delta Ct}$ method, the levels of RNA normalized to GAPDH or U6 were calculated.

CCK8 assay

Cell viability was detected by CCK8 assay. Cells (50,000/mL) were seeded and incubated in 96 well plate. 15 μL CCK8 solutions (Dojindo, Shanghai, China) were added. 2 hours later, the results were assessed by a microtitre plate reader (BioTek, Winooski, VT, USA) at 450 nm. Adriamycin purchased from MedChemExpress (USA) was incubated with cells at different concentrations.

Edu assay

AML cells were treated with 100 μL of Edu solution (20 μM, kFluor555 Click-iT EdU, Keygen BioTECH, Nanjing, China) in 96 well plate for 2 h at 37°C with 5% CO_2. After washing, cells were fixed by 4% paraformaldehyde and then 1% triton 100 for 45 min. Hoechst solution (Keygen BioTECH) were used to stain nuclei. The images were collected by fluorescence microscope (Leica, Wetzlar, Germany).

Apoptosis detection

Annexin V-FITC/PI staining assay kit (Vazyme, Nanjing, China) was used to determine the apoptosis rates. Cells were diluted in binding buffer (100 μL) and then cultured with probes for 10 min. After resuspending with 300 μL of binding buffer, the fluorescence was examined

Table 2. The primers sequence

	Forward	Reverse
GAPDH	5'-TCCGTGGTCCACGAGAACT-3'	5'-GAAGCATTTGCGGTGGACGAT-3'
circMYC	5'-CTCACAGCCCACTGGTCCTC-3'	5'-TCCAGCAGAAGGTGATCCAG-3'
miR-516a-5p	5'-CTCAACTGGTGTCGTGGAGTCGGCAATTCAGTTGAGGAAAGTGC-3'	5'-ACACTCCAGCTGGGTTCTCGAGGAAAGAAGC-3'
AKT3	5'-ATGAGCGATGTTACCATTGT-3'	5'-CAGTCTGTCTGCTACAGCCTGGATA-3'
U6	5'-CTCGCTTCGGCAGCACA-3'	5'-AACGCTTCACGAATTTGCGT-3'

by a flow cytometry (BD, CA, USA). The results were analyzed by FlowJo software (version 8.8.6; Tree Star).

Western blotting

The protein extraction (RIPA buffer, ThermoFisher Scientific, Waltham, MA, USA), concentration determination (BCA protein assay kit, ThermoFisher Scientific), separation and transferring to nitrocellulose filter membrane (Millipore, Boston, USA), incubation with BSA and antibodies were conducted according to manufacturer instruction. The primary antibodies for PCNA, Bcl2, caspase 3 (diluted at 1:1500; CST, USA) and β-actin (Santacruz, USA) were incubated at 4°C for 12 h. The secondary antibodies were obtained from Proteintech (USA). Protein expression was detected by ECL system (Amersham Pharmacia, Piscataway, NJ, USA).

XF cell mito stress test

The mitochondria function was evaluated by oxygen consumption rate (OCR). Mito Stress Test Kit (Seahorse, USA) was used to measure OCR in real-time by Seahorse Analyser (Agilent Technologies, USA) following manufacturer's instruction [14].

Fluorescence in situ hybridization (FISH)

The localization of circMYC was verified by FISH assay according to the protocol of the Fluorescent *In Situ* Hybridization Kit (Geneseed, China). DAPI was used to stain cell nuclei, and images were photographed under a fluorescence microscope (Leica). U6 and GAPDH were applied as control.

Bioinformation analysis

For interaction prediction, Starbase 2.0 (http://starbase.sysu.edu.cn/starbase2/), circBank (http://www.circbank.cn/) and circinteractome (https://circinteractome.irp.nia.nih.gov/) were used.

RNA pull-down assay

Cells were collected and lysed. MiR-516a-5p was biotinylated and the normal control was oligo probe. The miR-516a-5p probe (Tsingke, Wuhan, China) and streptavidin magnetic beads (Life Technologies, USA) were co-incubated for 2 h, which were then incubated with cell lysate at 4°C for 12 h. After washing twice, Trizol reagent (Takara, Otsu, Japan) was used for collection and the production was analyzed by RT-qPCR assay.

RNA immunoprecipitation (RIP) assay

In RIP assay, an EZ-Magna RIP kit (Millipore, USA) was used. The magnetic beads with antibody targeting Ago2 or IgG were added into cell lysis, as well as RIP buffer. Then, cell lysis was incubated with proteinase K, and the precipitated RNA was verified by PCR.

Dual-luciferase report (DLR) assay

To examine whether miR-516a-5p targeted circMYC or AKT3 directly, circMYC-WT, circMYC-MUT, AKT3-WT and AKT3-MUT were established in the pmiR-GLO dual-luciferase target expression vectors, which were obtained from Promega (Madison, WI, USA). The assays were described previously [15]. When cell confluence reached 60-75%, cells were co-transfected with reporter vectors and miR-NC or miR-516a-5p mimic using Lipofectamine 2000 (Invitrogen). Then the Dual-Luciferase Reporter Assay System (Promega) was used to detect the luciferase activity after 48 h.

Statistical analysis

SPSS 18.0 was used for the statistical analyses, and data were shown as the mean ± SD from at least three independent experiments.

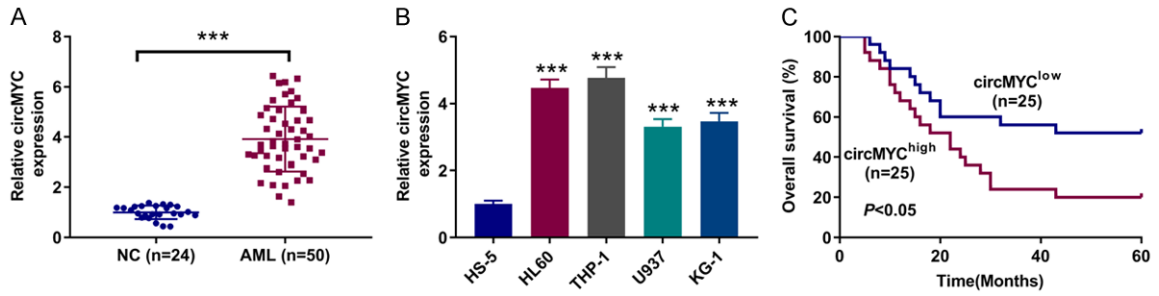

Figure 1. CircMYC was upregulated in AML. A. CircMYC was determined by RT-qPCR in the clinical specimens of AML patients (n=50) and healthy donors (NC, n=24). B. The expression of circMYC in different AML cell lines (HL60, THP-1, U937 and KG1) and normal bone marrow stomal cell line (HS5) were determined by RT-qPCR. C. The overall survival (OS) rates in AML patients with different levels of circMYC. All data are presented as mean ± SD (n=3). ***P<0.001.

The results were analyzed statistically using the analysis of variance and post hoc Student-Newman-Keuls test at a significance level of P<0.05.

Results

The expression of circMYC was enhanced in AML

First, the expression of circMYC was determined in clinical specimens of AML patients (n=50) and healthy donors (NC, n=24). Compared with PBMCs derived from healthy donors (NC), the level of circMYC was significantly up-regulated in PBMCs derived from AML patients (**Figure 1A**). The increased expression of circMYC was also observed in several AML cell lines, including HL60, THP-1, U937 and KG1, compared to that in HS5 which is a normal bone marrow stomal cell line (**Figure 1B**). Among them, the expression of circMYC was highest in HL60 and THP-1 cells, which were selected for further research. Besides, the overall survival (OS) rates were decreased in AML patients with higher level of circMYC (**Figure 1C**). All in all, circMYC was increased in AML cells, indicating a poor prognosis in AML patients.

Decreased expression of circMYC suppressed cell proliferation and promoted cell apoptosis

To verify the function of circMYC, different types of sh-circMYC were transfected into cells. The expression of circMYC was examined to verify the silence effect (**Figure 2A**). circMYC silencing significantly decreased the viability of HL60 and THP-1 cells (**Figure 2B**). Also, the EdU assay indicated that sh-circMYC suppressed the proliferation of HL60 and THP-1 cells (**Figure 2C**). On the other hand, the cell apoptosis rate was increased after circMYC silencing (**Figure 2D**). In **Figure 2E**, sh-circMYC decreased the levels of PCNA and Bcl2, while upregulated the expression of cleaved-caspase 3, suggesting the anti-apoptotic role of circMYC. Besides, sh-circMYC could increase the sensitivity of HL60 and THP-1 cells to adriamycin, a chemotherapy drug (**Figure 2F**). All these results indicated that circMYC promoted cell proliferation and suppressed cell apoptosis.

Silencing circMYC suppressed mitochondrial respiration of AML cells

Due to the anti-apoptotic role of circMYC, we then explored its impact on mitochondrial respiration. Mitochondrial oxidative phosphorylation was evaluated by OCR in HL60 and THP-1 cells transfected with sh-circMYC or sh-NC. As expected, compared with sh-NC group, OCR was decreased in sh-circMYC group (**Figure 3A**). Simultaneously, we observed that sh-circMYC could significantly decrease the basal respiration and maximal respiration (**Figure 3B**), suggesting that circMYC played a role in maintaining mitochondrial respiration in AML cells.

CircMYC was a direct target of miR-516a-5p

To deeply investigate the role of circMYC, its downstream effectors were identified. First, we demonstrated that circMYC was mostly localized in the cytoplasm (**Figure 4A**). Using prediction software including Starbase 2.0, circBank and circinteractome, we found that miR-516a-5p and miR-520h may potentially target circMYC (**Figure 4B**). However, circMYC only interacted with miR-516a-5p but not miR-520h

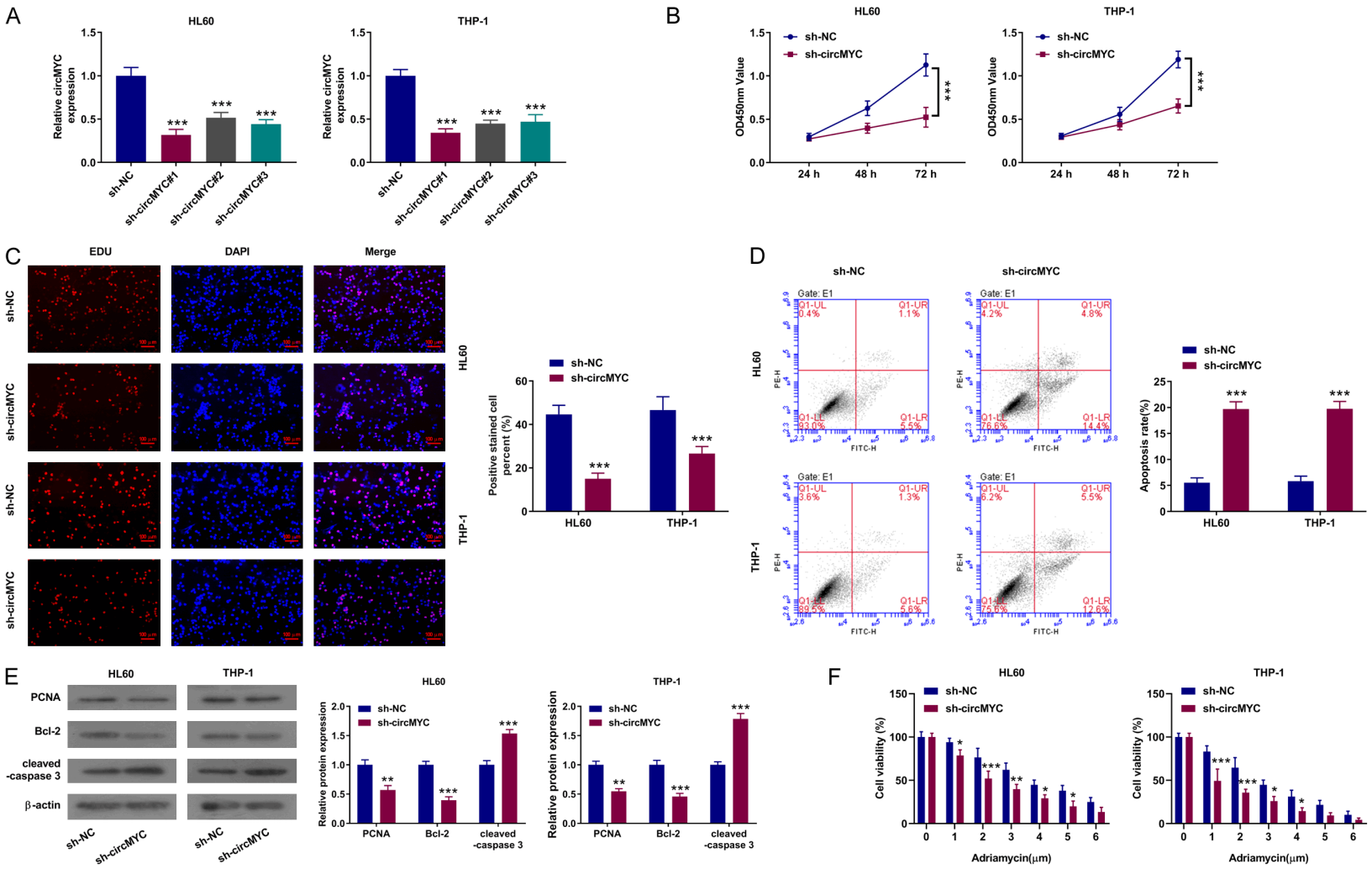

Figure 2. The effects of circMYC on cell proliferation and apoptosis in AML cells. A. CircMYC was determined by RT-qPCR after sh-circMYC#1, #2, #3 transfected into cells. B. Cell viability was detected by CCK8 assay at 24 h, 48 h, and 72 h after transfected with sh-circMYC. C. Cell proliferation was determined by EdU assay after transfected with sh-circMYC. Scale bar: 100 μM. 100× magnification. D. Cell apoptosis was verified by annexin V-FITC/PI staining assay after transfected with sh-circMYC. E. PCNA, Bcl-2 and cleaved-caspase 3 were detected by western blot after transfected with sh-circMYC. F. Cell viability after treating sh-circMYC and Adriamycin was assessed by CCK8 assay. All data are presented as mean ± SD (n=3). *P<0.05, **P<0.01, ***P<0.001.

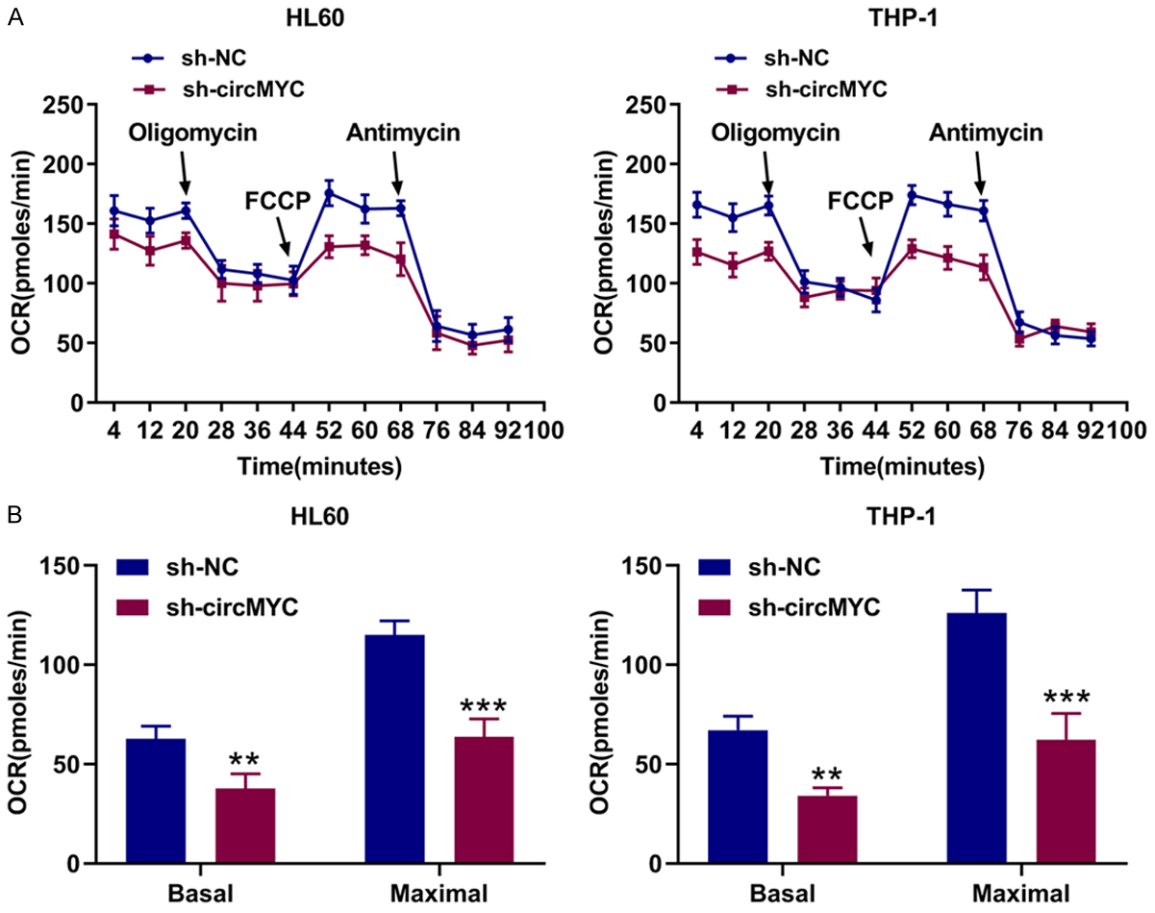

Figure 3. The effects of circMYC on mitochondrial respiration. OCR (A), basal respiration and maximal respiration (B) were assessed using a Seahorse XFp Cell Mito Stress Test kit. All data are presented as mean ± SD (n=3). **P<0.01, ***P<0.001.

(**Figure 4C**). We further confirmed the binding site between miR-516a-5p and circMYC by circinteractome (**Figure 4D**). MiR-516a-5p overexpression inhibited the luciferase activity of circMYC-WT, while the inhibitory effect was blocked by the mutated circMYC binding sites (**Figure 4E**). What's more, RIP assay proved the relationship between miR-516a-5p and circMYC (**Figure 4F**). After silencing circMYC, miR-516a-5p was dramatically increased in both cells (**Figure 4G**). All in all, circMYC was the target of miR-516a-5p and negatively associated with miR-516a-5p.

Overexpression of miR-516a-5p exerted an antitumor effect in AML cells

We further verified the mechanism of miR-516a-5p. Compared with HS-5 cells, miR-516a-5p was reduced in AML cell lines, including HL60, THP-1, U937 and KG1 (**Figure 5A**), indicating a negative correlation between miR-516a-5p and tumor malignancy. Then miR-516a-5p mimics were used to increase miR-516a-5p level (**Figure 5B**). In **Figure 5C**, miR-516a-5p overexpression suppressed cell viability, proliferation (**Figure 5D**), and induced apoptosis (**Figure 5E**) in HL60 and THP-1 cells. Also, miR-516a-5p mimics increased cleave-caspase 3, and reduced the expression of PCNA and Bcl2 (**Figure 5F**). In addition, miR-516a-5p mimics increased the sensitivity of HL60 and THP-1 cells to adriamycin (**Figure 5G**). Furthermore, OCR, basal respiration and maximal respiration were decreased both in HL60 and THP-1 cells transfected with miR-516a-5p mimic (**Figure 5H**, **5I**). These results confirmed the antitumor effects of miR-516a-5p.

AKT3 was targeted by miR-516a-5p

Next, the downstream target of miR-516a-5p was investigated by searching Starbase 2.0

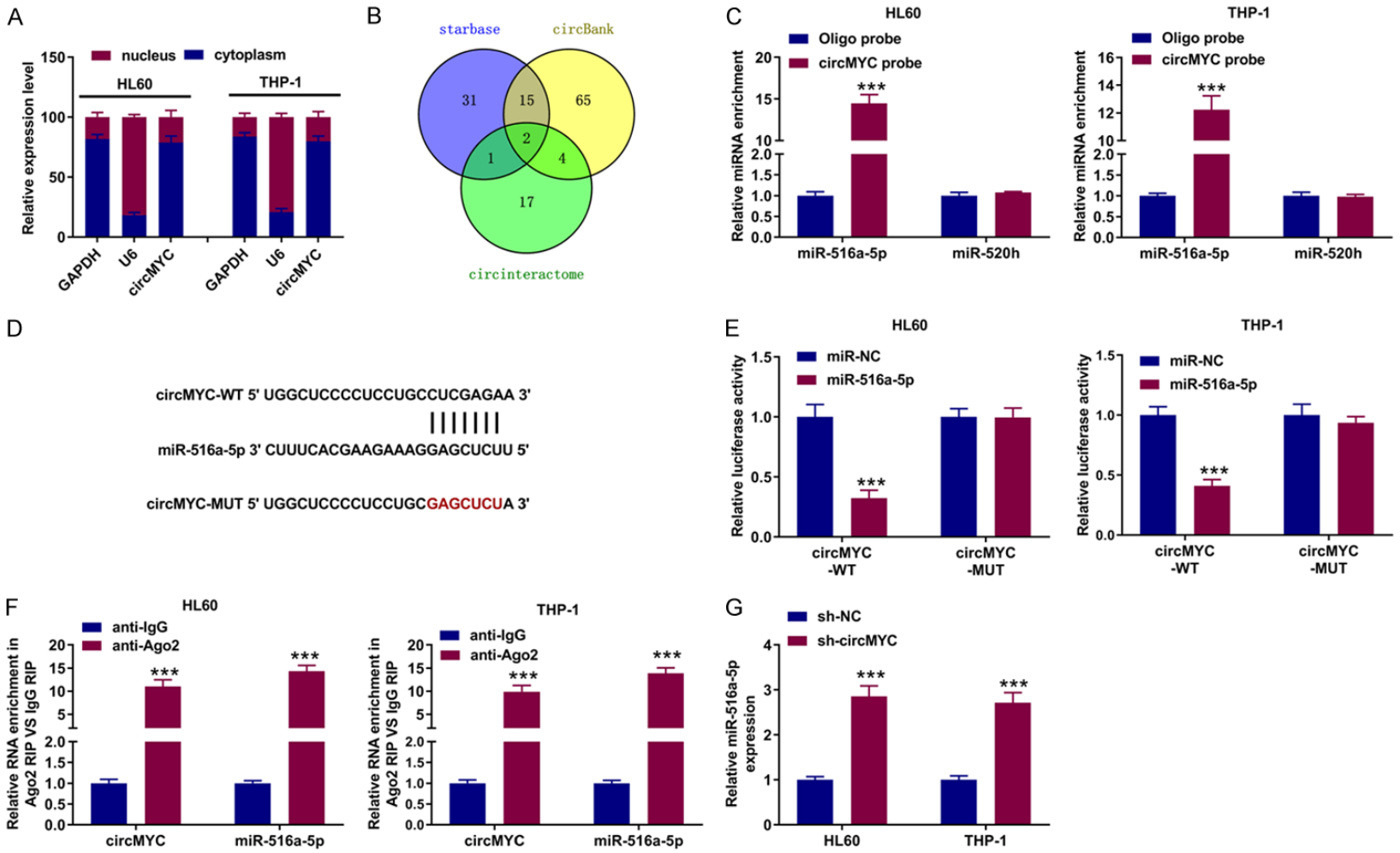

Figure 4. miR-516a-5p targeted circMYC. A. The subcellular localization of circMYC in HL60 and THP-1 cells was determined by FISH assay. B. Venn diagram of the targeting miRNAs of circMYC after predication. C. The interaction between circMYC and miR-516a-5p or miR-520h was determined by RNA-pull down. D. The binding sites were predicted by circinteractome database. E. The binding site between circMYC and miR-516a-5p was verified by dual-luciferase reporter assay. F. The relationship between circMYC and miR-516a-5p was assessed by RIP assay. G. MiR-516a-5p was detected by RT-qPCR after sh-circMYC transfection. All data are presented as mean ± SD (n=3). ***P<0.001.

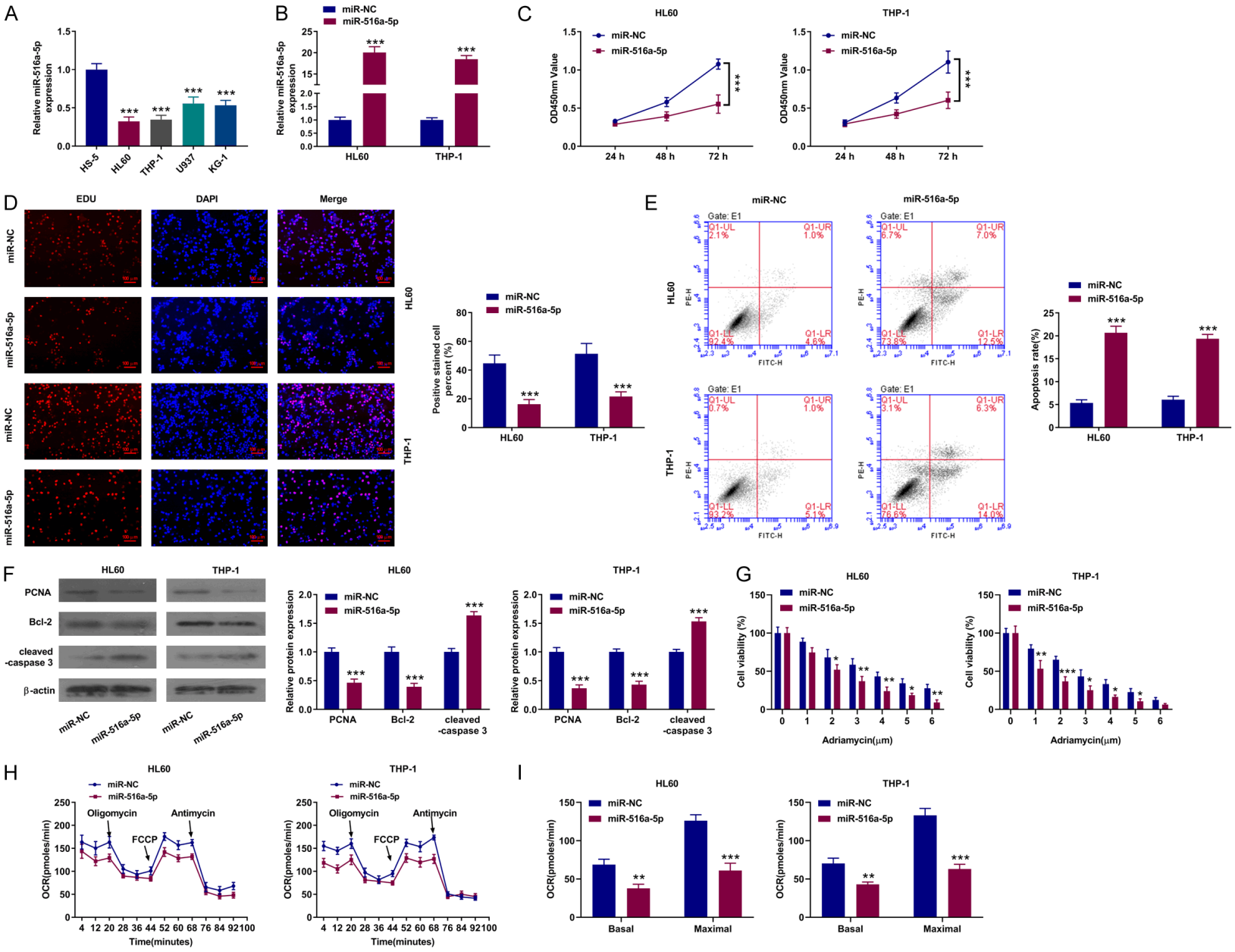
A
Relative miR-516a-5p expression
HS-5
HL60
THP-1
U937
KG-1
B
miR-NC
miR-516a-5p
Relative miR-516a-5p expression
HL60
THP-1
C
HL60
THP-1
miR-NC
miR-516a-5p
OD450nm Value
24 h
48 h
72 h
D
EDU
DAPI
Merge
miR-NC
miR-516a-5p
HL60
THP-1
Positive stained cell percent (%)
E
miR-NC
miR-516a-5p
Gate: E1
Q1-UL
Q1-UR
Q1-LL
Q1-LR
PE-H
FITC-H
Apoptosis rate(%)
F
HL60
THP-1
PCNA
Bcl-2
cleaved -caspase 3
β-actin
Relative protein expression
G
Cell viability (%)
Adriamycin(μm)
H
Oligomycin
FCCP
Antimycin
OCR(pmoles/min)
Time(minutes)
I
Basal
Maximal

Figure 5. The effects of miR-516a-5p on cell proliferation and apoptosis in AML cells. (A) MiR-516a-5p was detected by RT-qPCR in different AML cell lines (HL60, THP-1, U937 and KG1) and normal bone marrow stomal cell line (HS5). (B) MiR-516a-5p was detected by RT-qPCR after miR-516a-5p mimics transfection. (C) Cell viability was determined by CCK8 assay at 24 h, 48 h, and 72 h after miR-516a-5p mimics transfection. (D) Cell proliferation was detected by EdU assay after miR-516a-5p mimics transfection. Scale bar: 100 μM. 100× magnification. (E) Cell apoptosis was verified by annexin V-FITC/PI staining assay after miR-516a-5p mimics transfection. (F) PCNA, Bcl-2 and cleaved-caspase 3 were detected by western blot after miR-516a-5p mimics transfection. (G) Cell viability after treating miR-516a-5p mimics and Adriamycin was assessed by CCK8 assay. (H, I) OCR (H), basal respiration and maximal respiration (I) were assessed using a Seahorse XFp Cell Mito Stress Test kit. All data are presented as mean ± SD (n=3). *P<0.05, **P<0.01, ***P<0.001.

and it was found that miR-516a-5p could target AKT3 (**Figure 6A**). MiR-516a-5p mimics inhibited the luciferase activity in cells containing AKT3-WT, but not AKT3-MUT (**Figure 6B**). In addition, miR-516a-5p overexpression suppressed the protein level of AKT3 (**Figure 6C**). To investigate whether AKT3 was the downstream effector of circMYC/miR-516a-5p, a mi-516a-5p inhibitor was transfected into cells to silence mi-516a-5p (**Figure 6D**). **Figure 6E** showed that sh-circMYC inhibited the protein expression of AKT3. However, co-transfection with sh-circMYC and miR-516a-5p inhibitor reversed the protein level of AKT3 (**Figure 6E**). In conclusion, AKT3 was targeted by miR-516a-5p negatively and regulated by circMYC/miR-516a-5p axis.

CircMYC regulated cell proliferation, apoptosis and mitochondrial respiration by miR-516a-5p/AKT3 axis

After being transfected with AKT3 pcDNA3.1 plasmid, an increased expression of AKT3 was observed in HL60 and THP-1 cells, as displayed in **Figure 7A**. HL60 and THP-1 cells were co-transfected with sh-circMYC and miR-516a-5p inhibitor or AKT3 pcDNA3.1 plasmid, and the functions of circMYC/miR-516a-5p/AKT3 axis were verified. As shown in **Figure 7B-D**, the reduced cell viability and proliferation, and the enhanced cell apoptosis induced by sh-circMYC were reversed by miR-516a-5p knockdown or AKT3 overexpression. Consistently, sh-circMYC downregulated PCNA and Bcl2, and upregulated cleave-caspase 3, which could be rescued by miR-516a-5p knockdown or AKT3 overexpression (**Figure 7E**). Furthermore, sh-circMYC increased cell sensitivity to adriamycin, which could be abrogated by the transfection of miR-516a-5p inhibitor or AKT3 pcDNA3.1 plasmid (**Figure 7F**). The decreased basal respiration and maximal respiration were blocked after knockdown of miR-516a-5p or overexpression of AKT3 (**Figure 7G**). The schematic diagram of our research summarized in **Figure 8** demonstrates that miR-516a-5p could negatively target circMYC to inhibit the progression of AML by influencing cell viability, proliferation, apoptosis and mitochondrial respiration, which was negatively associated with AKT3. In summary, circMYC regulated the functions of AML cells by modulating miR-516a-5p/AKT3 axis.

Discussion

AML is a malignant neoplastic disease, showing unrestricted proliferation of immature myeloid cells in bone marrow and peripheral blood [16]. The vital roles of ncRNAs in AML have been emphasized [17, 18]. In this study, we found that circMYC was upregulated in AML cells and served as an oncogenic gene. What's more, circMYC was associated with poor prognosis and chemotherapy-resistance of AML. Knockdown of circMYC suppressed cell proliferation, induced apoptosis and reduced mitochondrial respiration in AML cells. Mechanistically, circMYC upregulated the expression of AKT3 by functioning as a sponge of miR-516a-5p. Thus, the regulated function of circMYC was achieved through miR-516a-5p/AKT3 axis.

In melanoma cells, circMYC was upregulated significantly and modulated cell proliferation [19]. In nasopharyngeal carcinoma (NPC), increased expression of circMYC was related to tumor size, migration and invasion, clinical stage and survival time. Briefly, overexpression of circMYC not only promoted cell proliferation, but also increased tumor radiotherapy resistance [13]. Although the role of circMYC has not been reported in AML, it is indicated that in multiple myeloma, circMYC promoted tumor recurrence and facilitated drug resistance [12]. Consistently, the oncogenic role of

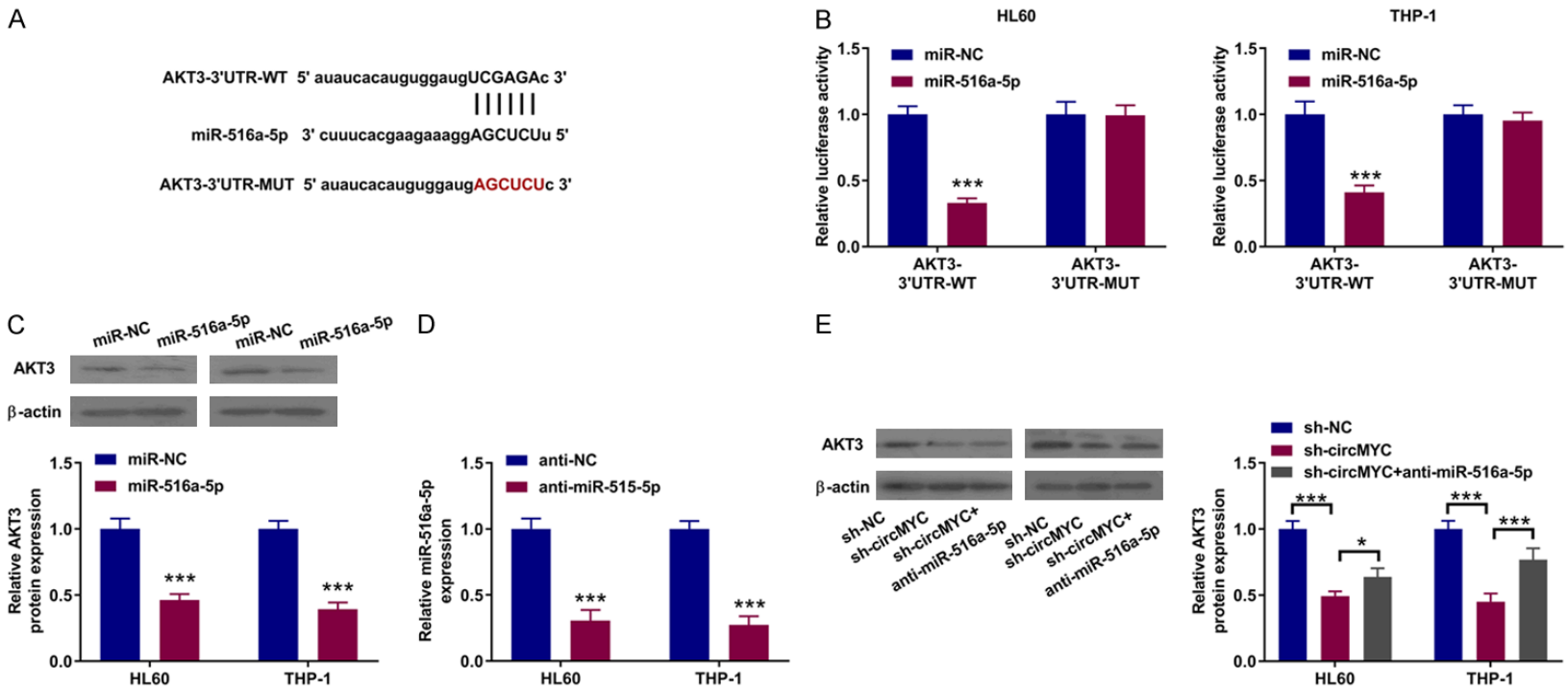

Figure 6. AKT3 targeted to miR-516a-5p. A. The predicted binding sites were obtained from Starbase 2.0. B. The binding relationship between miR-516a-5p and AKT3 was verified by dual-luciferase reporter assay. C. The protein expression of AKT3 was determined by western blot after miR-516a-5p mimics transfection. D. MiR-516a-5p was detected by RT-qPCR after miR-516a-5p inhibitor transfection. E. AKT3 was determined by western blot after sh-circMYC and/or miR-516a-5p inhibitor transfection. All data are presented as mean ± SD (n=3). *P<0.05, ***P<0.001.

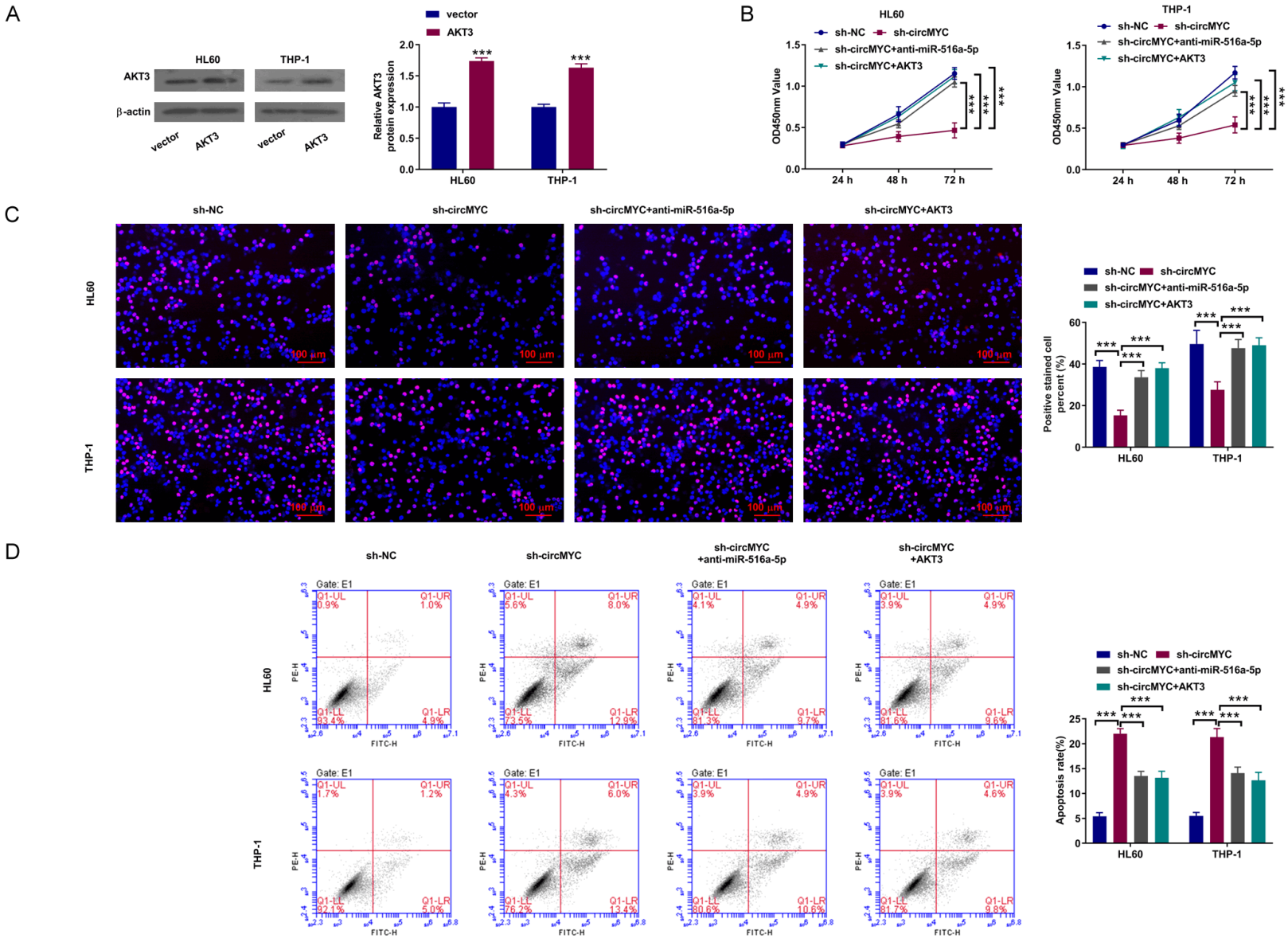
A
HL60
THP-1
AKT3
β-actin
vector
AKT3
vector
AKT3
Relative AKT3 protein expression
HL60
THP-1
B
HL60
sh-NC
sh-circMYC
sh-circMYC+anti-miR-516a-5p
sh-circMYC+AKT3
OD450nm Value
24 h
48 h
72 h
THP-1
C
sh-NC
sh-circMYC
sh-circMYC+anti-miR-516a-5p
sh-circMYC+AKT3
HL60
THP-1
100 μm
Positive stained cell percent (%)
D
sh-NC
sh-circMYC
sh-circMYC +anti-miR-516a-5p
sh-circMYC +AKT3
Gate: E1
Q1-UL
Q1-UR
Q1-LL
Q1-LR
PE-H
FITC-H
Apoptosis rate(%)

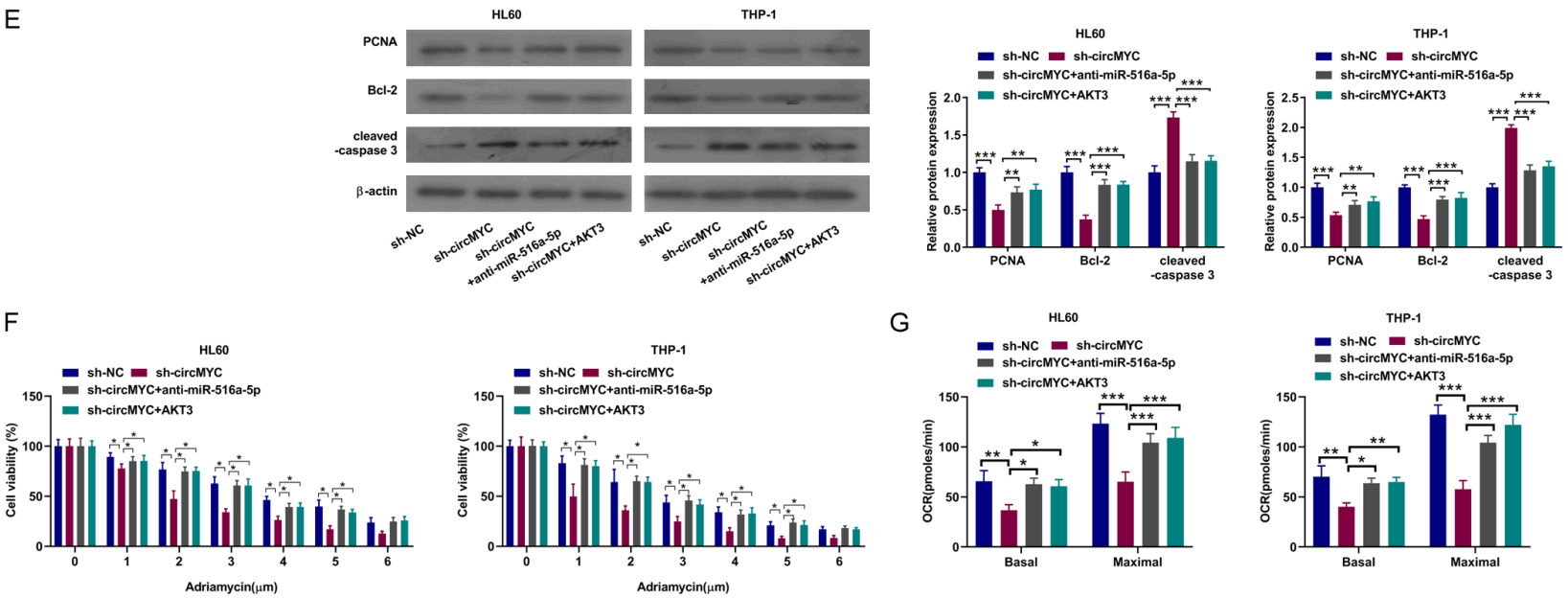

Figure 7. CircMYC regulated cell proliferation, apoptosis and mitochondrial respiration via miR-516a-5p/AKT3 axis. A. AKT3 was determined by western blot after AKT3 pcDNA3.1 plasmid transfection. B. Cell viability was detected by CCK8 assay at 24 h, 48 h, and 72 h after sh-circMYC and miR-516a-5p inhibitor or AKT3 pcDNA3.1 plasmid co-transfection. C. Cell proliferation was determined by EdU assay after sh-circMYC and miR-516a-5p inhibitor or AKT3 pcDNA3.1 plasmid co-transfection. Scale bar: 100 μM. 100× magnification. D. Cell apoptosis was verified by annexin V-FITC/PI staining assay after sh-circMYC and miR-516a-5p inhibitor or AKT3 pcDNA3.1 plasmid co-transfection. E. PCNA, Bcl-2 and cleaved-caspase 3 were detected by western blot after sh-circMYC and miR-516a-5p inhibitor or AKT3 pcDNA3.1 plasmid co-transfection. F. Cell viability was assessed by CCK8 assay after sh-circMYC and miR-516a-5p inhibitor or AKT3 pcDNA3.1 plasmid co-transfection. G. Basal respiration and maximal respiration were assessed using a Seahorse XFp Cell Mito Stress Test kit. All data are presented as mean ± SD (n=3). *P<0.05, **P<0.01, ***P<0.001.

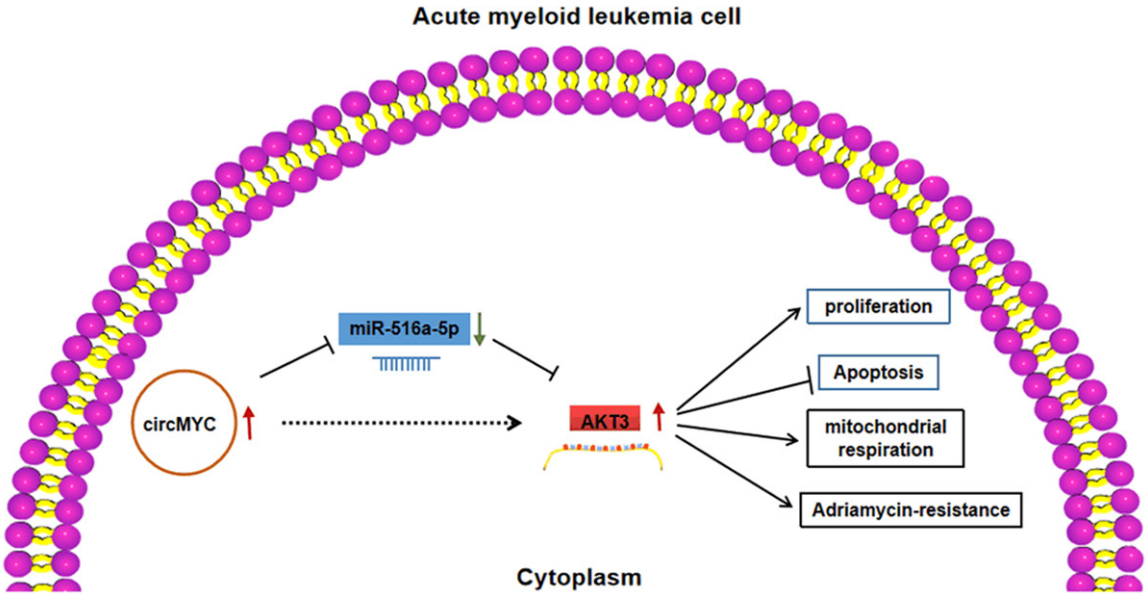

Figure 8. The schematic diagram of circMYC/miR-516a-5p/AKT3 axis.

circMYC was verified in our research. After knockdown of circMYC, cell viability and proliferation were reduced. Also, the decreased expression of circMYC was found to increase cell apoptosis, including regulating the expression of apoptosis related proteins and blocking mitochondrial respiration function. Therefore, our results showed that circMYC might be a novel biomarker and therapeutic target for AML.

CircRNA could regulate the expression of miRNAs by functioning as their sponge [20]. We found that circMYC was targeted by miR-516a-5p, and the expression of miR-516a-5p could be enhanced after circMYC knockdown. Importantly, the antitumor effect induced by circMYC knockdown was blocked by miR-516a-5p inhibitor, showing that miR-516a-5p was a tumor suppressor in AML. The antitumor effect of miR-516a-5p has been reported in many studies. For example, in non-small cell lung cancer, miR-516a-5p suppressed cell proliferation [21]. After sponging miR-516a-5p in hepatocellular carcinoma by circRNA_0001955, the tumorigenesis was enhanced [22]. Similarly, circRNA_103809 and circNCOR2 accelerated cancer progression by targeting miR-516a-5p and suppressing its expression in papillary thyroid cancer [23]. In these studies, the expression of miR-516a-5p was reduced in tumor cells and tissues, suggesting the relationship between the decreased miR-516a-5p level and poor prognosis. However, some studies have also found the opposite effect of miR-516a-5p, demonstrating that miR-516a-5p accelerated the progression of bladder cancer (BC) [24]. In BC cells, the increased miR-516a-5p was related to a phenotype with higher invasion ability, and the suppression of miR-516a-5p reduced the invasion and migration of BC cells both *in vivo* and *in vitro* [24]. Therefore, the specific role of miR-516a-5p needs to be analyzed for specific tumors in depth. Unfortunately, the limitation of this research is that we only proved the anti-tumor effect of miR-516a-5p *in vitro*. Further *in vivo* studies would be performed to deeply excavate the effect of miR-516a-5p on AML.

Many studies have found out that PI3K/AKT pathway was vital in tumor genesis and development, including the regulation of cell proliferation, apoptosis, metabolism, invasion and metastasis [25]. There are three subtypes of AKT, including AKT1, AKT2, and AKT3. AKT3 was discovered a few years ago and verified as an oncogene [26]. Previous studies showed that knockdown of AKT3 attenuated the proliferation of breast cancer cells [27]. In AML cells, it was also shown that AKT3 played an oncogenic role by increasing cell proliferation, promoting cell cycle and suppressing apoptosis [28]. In this research, miR-516a-5p could tar-

get AKT3 and decrease the expression of AKT3. As the downstream of circMYC, the function of sh-circMYC could be blocked by AKT3 overexpression, suggesting that the effects of circMYC was mediated by AKT3.

In conclusion, circMYC can be used as a potential biomarker for AML. Decreased expression of circMYC could suppress the progression of AML by regulating miR-516a-5p/AKT3 axis. In this study, we not only suggested the regulatory effect among circMYC, miR-516a-5p and AKT3, but also provided a new therapeutic direction for AML treatment, which are the prospects of this study.

Acknowledgements

Natural Science Foundation of Shenzhen University General Hospital.

Disclosure of conflict of interest

None.

Abbreviations

AML, acute myeloid leukemia; OCR, oxygen consumption rate; DLR, dual-luciferase reporter; RIP, RNA immunoprecipitation; FAB, French-American-British; As2O3, arsenic trioxide; allo-BMT, allogeneic bone marrow transplantation; miRNAs, microRNAs; ncRNAs, non-coding RNA; circRNAs, circular RNAs; lncRNAs, long noncoding RNAs; PBMCs, peripheral blood mononuclear cells; ATCC, American type culture collection; NC, negative control; RT-qPCR, Quantitative reverse transcription PCR; OS, overall survival; NPC, nasopharyngeal carcinoma; BC, bladder cancer.

Address correspondence to: Min Jiang, Department of Pediatrics, Shenzhen University General Hospital, No. 1098 Xueyuan Road, Nanshan District, Shenzhen 518055, Guangdong Province, China. Tel: +86-0755-21839018; Fax: +86-0755-21839999; E-mail: dtjiangmin@163.com

References

[1] Khwaja A, Bjorkholm M, Gale RE, Levine RL, Jordan CT, Ehninger G, Bloomfield CD, Estey E, Burnett A, Cornelissen JJ, Scheinberg DA, Bouscary D and Linch DC. Acute myeloid leukaemia. Nat Rev Dis Primers 2016; 2: 16010.

[2] Rose D, Haferlach T, Schnittger S, Perglerova K, Kern W and Haferlach C. Subtype-specific patterns of molecular mutations in acute myeloid leukemia. Leukemia 2017; 31: 11-17.

[3] Conneely SE and Stevens AM. Advances in pediatric acute promyelocytic leukemia. Children (Basel) 2020; 7: 11.

[4] Almond LM, Charalampakis M, Ford SJ, Gourevitch D and Desai A. Myeloid sarcoma: presentation, diagnosis, and treatment. Clin Lymphoma Myeloma Leuk 2017; 17: 263-267.

[5] Anguille S, Van de Velde AL, Smits EL, Van Tendeloo VF, Juliusson G, Cools N, Nijs G, Stein B, Lion E, Van Driessche A, Vandenbosch I, Verlinden A, Gadisseur AP, Schroyens WA, Muylle L, Vermeulen K, Maes MB, Deiteren K, Malfait R, Gostick E, Lammens M, Couttenye MM, Jorens P, Goossens H, Price DA, Ladell K, Oka Y, Fujiki F, Oji Y, Sugiyama H and Berneman ZN. Dendritic cell vaccination as postremission treatment to prevent or delay relapse in acute myeloid leukemia. Blood 2017; 130: 1713-1721.

[6] Liu Y, Cheng Z, Pang Y, Cui L, Qian T, Quan L, Zhao H, Shi J, Ke X and Fu L. Role of microRNAs, circRNAs and long noncoding RNAs in acute myeloid leukemia. J Hematol Oncol 2019; 12: 51.

[7] Liao Q, Wang B, Li X and Jiang G. miRNAs in acute myeloid leukemia. Oncotarget 2017; 8: 3666-3682.

[8] Wallace JA and O'Connell RM. MicroRNAs and acute myeloid leukemia: therapeutic implications and emerging concepts. Blood 2017; 130: 1290-1301.

[9] Bartel DP. MicroRNAs: target recognition and regulatory functions. Cell 2009; 136: 215-233.

[10] Lin JF, Zeng H and Zhao JQ. MiR-212-5p regulates the proliferation and apoptosis of AML cells through targeting FZD5. Eur Rev Med Pharmacol Sci 2018; 22: 8415-8422.

[11] Cheng Y, Su Y, Wang S, Liu Y, Jin L, Wan Q, Liu Y, Li C, Sang X, Yang L, Liu C and Wang Z. Identification of circRNA-lncRNA-miRNA-mRNA competitive endogenous RNA network as novel prognostic markers for acute myeloid leukemia. Genes (Basel) 2020; 11: 868.

[12] Luo Y and Gui R. Circulating exosomal CircMYC is associated with recurrence and bortezomib resistance in patients with multiple myeloma. Turk J Haematol 2020; 37: 248-262.

[13] Luo Y, Ma J, Liu F, Guo J and Gui R. Diagnostic value of exosomal circMYC in radioresistant nasopharyngeal carcinoma. Head Neck 2020; 42: 3702-3711.

[14] Wang L, Pavlou S, Du X, Bhuckory M, Xu H and Chen M. Glucose transporter 1 critically controls microglial activation through facilitating glycolysis. Mol Neurodegener 2019; 14: 2.

[15] Zhu YJ and Jiang DM. LncRNA PART1 modulates chondrocyte proliferation, apoptosis, and

extracellular matrix degradation in osteoarthritis via regulating miR-373-3p/SOX4 axis. Eur Rev Med Pharmacol Sci 2019; 23: 8175-8185.
[16] Magina KN, Pregartner G, Zebisch A, Wölfler A, Neumeister P, Greinix HT, Berghold A and Sill H. Cytarabine dose in the consolidation treatment of AML: a systematic review and meta-analysis. Blood 2017; 130: 946-948.
[17] Liu Y, Cheng Z, Pang Y, Cui L, Qian T, Quan L, Zhao H, Shi J, Ke X and Fu L. Role of microRNAs, circRNAs and long noncoding RNAs in acute myeloid leukemia. J Hematol Oncol 2019; 12: 51.
[18] Fatica A. Noncoding RNAs in acute myeloid leukemia: from key regulators to clinical players. Scientifica (Cario) 2012; 2012: 925758.
[19] Jin C, Dong D, Yang Z, Xia R, Tao S and Piao M. CircMYC regulates glycolysis and cell proliferation in melanoma. Cell Biochem Biophys 2020; 78: 77-88.
[20] Rong D, Sun H, Li Z, Liu S, Dong C, Fu K, Tang W and Cao H. An emerging function of circRNA-miRNAs-mRNA axis in human diseases. Oncotarget 2017; 8: 73271-73281.
[21] Ye XY, Xu L, Lu S and Chen ZW. MiR-516a-5p inhibits the proliferation of non-small cell lung cancer by targeting HIST3H2A. Int J Immunopathol Pharmacol 2019; 33: 2058738419841481.
[22] Yao Z, Xu R, Yuan L, Xu M, Zhuang H, Li Y, Zhang Y and Lin N. Circ_0001955 facilitates hepatocellular carcinoma (HCC) tumorigenesis by sponging miR-516a-5p to release TRAF6 and MAPK11. Cell Death Dis 2019; 10: 945.
[23] Luan S, Fu P, Wang X, Gao Y, Shi K and Guo Y. Circular RNA circ-NCOR2 accelerates papillary thyroid cancer progression by sponging miR-516a-5p to upregulate metastasis-associated protein 2 expression. J Int Med Res 2020; 48: 300060520934659.
[24] Chang Y, Jin H, Li H, Ma J, Zheng Z, Sun B, Lyu Y, Lin M, Zhao H, Shen L, Zhang R, Wu S, Lin W, Lu Y, Xie Q, Zhang G, Huang X and Huang H. MiRNA-516a promotes bladder cancer metastasis by inhibiting MMP9 protein degradation via the AKT/FOXO3A/SMURF1 axis. Clin Transl Med 2020; 10: e263.
[25] Wang L, Huang D, Jiang Z, Luo Y, Norris C, Zhang M, Tian X and Tang Y. Akt3 is responsible for the survival and proliferation of embryonic stem cells. Biol Open 2017; 6: 850-861.
[26] Hinz N and Jucker M. Distinct functions of AKT isoforms in breast cancer: a comprehensive review. Cell Commun Signal 2019; 17: 154.
[27] Grabinski N, Mollmann K, Milde-Langosch K, Muller V, Schumacher U, Brandt B, Pantel K and Jucker M. AKT3 regulates ErbB2, ErbB3 and estrogen receptor alpha expression and contributes to endocrine therapy resistance of ErbB2(+) breast tumor cells from Balb-neuT mice. Cell Signal 2014; 26: 1021-1029.
[28] Nie ZY, Zhao MH, Cheng BQ, Pan RF, Wang TR, Qin Y and Zhang XJ. Tanshinone IIA regulates human AML cell proliferation, cell cycle, and apoptosis through miR-497-5p/AKT3 axis. Cancer Cell Int 2020; 20: 379.